Surface-barrier Structures Au/*n*-CdS: Fabrication and Electrophysical Properties

R. Petrus[1], H. Ilchuk[1], A. Kashuba[1,2], I. Semkiv[1], E. Zmiiovska[1], F. Honchar[1], R. Lys[2]

[1] *Lviv Polytechnic National University, General Physics Department, 12, S. Bandera St., 79013 Lviv, Ukraine*
[2] *Ivan Franko National University of Lviv, Faculty of Electronics and Computer Technologies, 107, Tarnavsky St., 79005 Lviv, Ukraine*

The results of the electrophysical properties study of Au/n-CdS surface-barrier structures (SBS) obtained by radio frequency (RF) magnetron sputtering are presented. It was established that CdS films crystallize in the space group *P63mc*. The results of I-V characteristics investigation for films in the dark and under illumination are presented. The ideality factor, the potential barrier height on the metal contact, the saturation current, the resistivity, the rectification factor and the built-in potential of the structure in the dark and under illumination are calculated based on the behavior of the I-V characteristic. In the process of illumination by a solar radiation simulator of the structure from the side of Au, the rectification factor k increases from 3 to 22 in comparison with the dark I-V characteristic. The multistage tunneling and recombination processes with the involvement of the surface states at the metallurgical Au/*n*-CdS interface is a dominant mechanism of charge transfer which established from the dark I-V characteristics of the forward-bias voltages. For the illuminated I-V characteristics, for biases < 0.6 V the tunneling and recombination mechanisms of the charge transport are dominant, and for biases > 0.6 V, the contribution of the tunneling mechanism increases. At reverse voltages for the dark and illuminated I-V characteristics, for biases < 0.3 V the dominant mechanism of charge transport is tunneling of charge carriers or currents confined by the space charge in the saturation mode of the carrier rate, and for biases > 0.3 V – currents confined by the space charge in the mobility mode. From the photoconductivity (PC) investigation, the band gap and absorption dependencies of the fabricated film were established.

Keywords: Magnetron sputtering, Thin films, CdS, Schottky barrier, Photoconductivity.

1. INTRODUCTION

Cadmium sulfide (CdS) is a promising semiconductor material for optoelectronic devices due to the room temperature band gap value (2.5 eV) which are in the visible spectrum of radiation. It was established that CdS films crystallize in the space group *P63mc* [1]. In particular, CdS is the most used material as an optical window in heterojunction solar cells based on CdTe and CIGS [2]. Electrophysical properties of cadmium sulfide layers obtained by RF magnetron sputtering for its future optimization as a window layer for thin film solar cells based on CdS/CdTe and CdS/CIGS were studied. Au/n-CdS surface-barrier structures (SBS) were fabricated for a quick and convenient way of identifying semiconductor films, investigating their physical properties and verifying the capability of fabricating photoconductors based on them.

2. EXPERIMENTAL DETAILS

CdS films were obtained by RF magnetron sputtering (13.6 MHz) using VUP-5M (Selmi) by method [1]. 16×8×1.1 mm³ glass\ITO (NANOCS IT100-111-25, 100 Ohm/sq) substrates were used for the deposition of CdS thin films. Before the CdS film deposition, the substrate surface was cleaned by boiling in a high purity CCl_4 solution during 0.25 h. The ITO layer provides a transparent electrical ohmic contact to the CdS film.

The target for RF magnetron sputtering was monocrystalline CdS disk with 99.999 % purity, 1 mm thickness and 40 mm diameter. The distance between the target and the substrate during the deposition process was 90 mm. Sputtering was carried out in the argon (Ar) atmosphere with its pressure of 1.0-1.3 Pa. The power of the RF magnetron was maintained at 30 W and the substrate temperature was 300 °C. The average film deposition rate was 4 Å/s.

For identifying the obtained cadmium sulfide film by the electro-optical method, the Schottky barrier type SBS were fabricated. This was done by depositing the 200 nm thickness gold (Au) layer on the CdS film without any post-deposition processing. The gold deposition as a barrier contact was carried out by a direct current magnetron sputtering using a gold target with 99.99 % purity. The distance between the target and the substrate during the deposition process was 90 mm. The average film deposition rate was 4 Å/s, the beginning and end of the process were controlled by a moving plate. Before the deposition, the working chamber was vacuumed. The residual gas pressure in the working chamber was $1 \cdot 10^{-4}$ Pa due to using in the steam-oil pump a "Polyphenyl ether 5Ф4Э" diffusion liquid which is characterized by a low $(9 \cdot 10^{-7}$ Pa) value of partial pressure. In order to prevent the entering working fluid vapor into the vacuum chamber, the Liquid Nitrogen Trap was used during the process of deposition. Sputtering was carried out in the argon (Ar) atmosphere with its pressure of 0.5 Pa. The DC magnetron discharge current was maintained at 30 mA and the substrate temperature was 120 °C. A 300 Watt power tungsten high-temperature heater was used to heat the substrates. The regulation of the heating and cooling rate and the temperature conditions of deposition was performed by PID controller.

The area of obtained barrier contacts was 2.5 mm². Gold films are characterized by high adhesion to the CdS semiconductor layer.

3. RESULTS AND DISCUSSION

We deposited CdS thin film on ITO/glass substrate by RF magnetron sputtering. The resulting film possessed a homogeneous light orange color, which is typical for a compound of cadmium sulfide. According to the analysis of the diffractograms for CdS (not shown), it was established that the film is single-phase, and the spatial group of the CdS compound is $P63mc$ [1].

Au/n-CdS SBS used for electrophysical and photovoltaic measurements are shown in Fig. 1. Four pairs of contacts were investigated to determine the reproducibility of the *I-V* characteristic across the entire film area. The *I-V* characteristic of the Au/n-CdS structure was measured at room temperature using the HP 4145A Semiconductor Parameters Analyzer. The measurement results of the *I-V* characteristic for various contacts are reproduced with an accuracy of 0.98. This suggests that the film has the same thickness across the entire area. Registered by the thermal probe method, the CdS thin film has n-type conductivity.

Created Au/n-CdS structures have a sufficiently high straightening property, which testifies to the formation of the high-quality metal-semiconductor junction. In this work, a dark *I-V* characteristic (Fig. 2, curve 1) and *I-V* characteristic obtained in the illumination from the side of the barrier contact Au (curve 2) are shown. The irradiation was carried out by a solar radiation simulator SF-150-C, which provided a power density emitted $F = 1000$ W/m^2.

Since ITO and CdS can form a good ohmic contact with each other, there is no obvious potential barrier on their boundary. According to the Schottky-Mott theory, the space charge region is formed due to the difference between work function of the metal (Au) $\Phi_{Au} = 5.38$ eV [3] and electron affinity of the semiconductor (CdS) $\chi_{CdS} = 4.8$ eV [4]. As a result, the flux of electrons from n-CdS to Au occurs and the Fermi level is equalized under thermal equilibrium conditions (see Fig. 2, inset). From Fig. 2 we see that the obtained SBS exhibit a legible rectification, at which the throughput direction corresponds to the negative polarity of the reverse bias on the ohmic contact of the ITO. The rectification factor k of the Au/n-CdS SBS was determined for illuminated and dark volt-ampere characteristics as a ratio between the forward and reverse currents at a bias of $U = \pm 0.5$ V. In the process of illumination (1000 W/m^2) of the structure from the side of Au, the rectification factor k increases from $k = 3$ to $k = 22$ in comparison with the dark *I-V* characteristic.
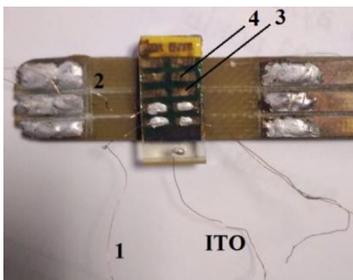

Fig. 1 – Photograph of the experimental Au/CdS SBS on the ITO/glass substrate: ITO – ohmic contact with CdS film, 1-4 – barrier contacts Au

The built-in potential V_{bi} and the series resistance R_s for the dark and illuminated Au/n-CdS SBS at room temperature are calculated directly from the linear section of the straight-line *I-V* characteristic. A linear regression method was used to describe the curve $I = f(U)$ in the voltage range of larger values of the built-in potential V_{bi} and the linear equation $I = a + bU$ was obtained which intersects the abscissa axis at the coordinate point V_{bi}.

We observe (see Fig. 2) the high value of convergence of experimental data with a linear approximation $R_1^2 = 0.9953$ and $R_2^2 = 0.9955$ for dark and illuminated *I-V* characteristic, respectively, which indicates the high accuracy of the chosen calculation technique.
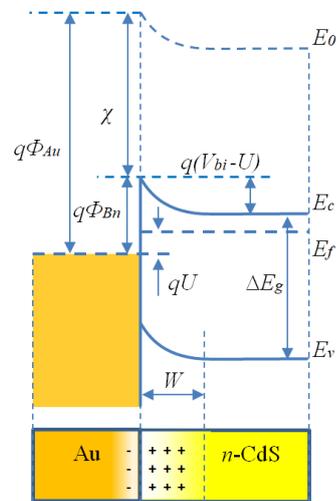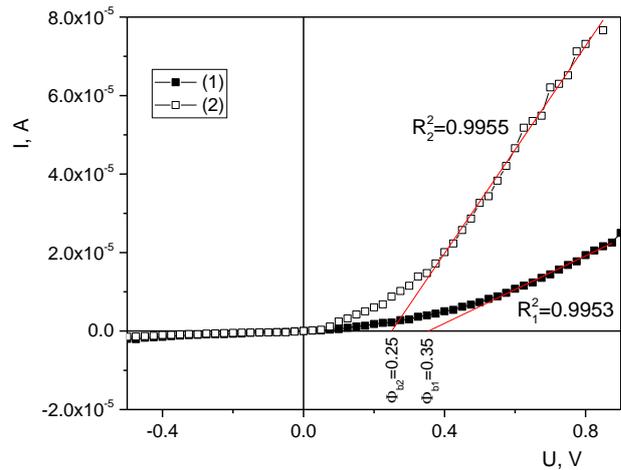

Fig. 2 – *I-V* characteristics of the Au/n-CdS structure obtained with the use of contact No. 1 (Fig. 1): 1 – dark, 2 – lighting. The inset shows a diagram of the ideal Schottky Au/n-CdS contact

The formula for determining the built-in potential is:

$$V_{bi} = -\frac{a}{b}. \tag{1}$$

The value of the series resistance R_s was determined from the slope of the straight line using the regression coefficient b by the expression:

$$R_s = \frac{1}{b}. \tag{2}$$

Among the main parameters that describe the stationary I-V characteristic of a Schottky contact are the height of the barrier $e\Phi_{Bn}$ for the electrons from the metal side, the ideality factor β, the series R_s and the shunting R_p resistances [5]:

$$I = I_0 \left(e^{\frac{qU}{\beta kT}} - 1 \right). \tag{3}$$

In the case of ideal metal-semiconductor contact, the ideality factor β is equal to one. However, experimentally, ideal Schottky contact can never be realized [4], therefore, the coefficient β, which is usually larger than one, takes into account series resistance, carrier recombination when crossing the space-charge region, and determines the predominant charge transfer mechanisms.

The value of the saturation current is given by the expression

$$I_0 = A \cdot ST^2 e^{\frac{q\Phi_{Bn}}{\beta kT}} \tag{4}$$

For the forward-bias voltages, at which $qU > 3kT$ in the equation (3), unit can be neglected:

$$I = I_0 \cdot e^{\frac{qU}{\beta kT}}, \tag{5}$$

$$\boldsymbol{ln}\, I = \boldsymbol{ln}\, I_0 + \frac{qU}{\beta kT} \tag{6}$$

From formula (6), we see that the graph $lnI = f(U)$ at constant temperature represents a straight line with the equation $y = A + Bx$, which intersects the axis of ordinates at the point $A = lnI_0$ and the slope coefficient of the straight line $B = \dfrac{q}{\beta kT}$.

Therefore, the saturation current value can be calculated by the formula:

$$I_0 = \boldsymbol{exp}\,(A), \tag{7}$$

and expression for the ideality factor is:

$$\beta = \frac{q}{kTB}. \tag{8}$$

From formula (4) we obtain an expression for calculating the potential-barrier height from the metal side $q\Phi_{Bn}$, in which there is an effective Richardson constant A^* and contact area S

$$q\Phi_{Bn} = kT \, \boldsymbol{ln} \left(\frac{A^* ST^2}{I_0} \right). \tag{9}$$

Absolute error of the potential-barrier height was calculated by the formula:

$$\Delta q\Phi_{Bn} = k \left[\boldsymbol{ln} \left(\frac{A^* ST^2}{I_0} \right) + 2 \right] \Delta T + \\ + kT \left(\frac{\Delta A^*}{A} + \frac{\Delta S}{S} + \frac{\Delta I_0}{I_0} \right). \tag{8}$$

The effective Richardson constant can be experimentally determined in the presence of temperature dependence of the *I-V* characteristic.

In the absence of the experimental values of A^*, in the calculation of the barrier height, the modified Richardson constant is often used [6]:

$$A^* = \frac{4\pi qm^* k^2}{h^3} = 120.173 \frac{A}{cm^2 \cdot K^2}. \tag{11}$$

The value of Φ_{Bn} is not very sensitive to the choice of A^*, since at room temperature 100 % increase in A^* will increase the Φ_{Bn} only by 0.018 V [4].

In Fig. 3, (curve 1), we see that the forward bias of *I-V* characteristic of the unlit (dark) Au/*n*-CdS on a semi-logarithmic scale $\boldsymbol{ln}\, I = f(U) \left(U > \dfrac{3kT}{q} \right)$ shows a single rectilinear portion indicating an exponential current dependence on the applied voltage. A large value of the ideality factor $\beta = 11.34$ (see Table 1) of the dark *I-V* characteristic can indicate that the dominant mechanism of charge transport in the region of forwarding biases is represented by multistage tunneling-recombination processes with the involvement of surface states at the Au/*n*-CdS [7].
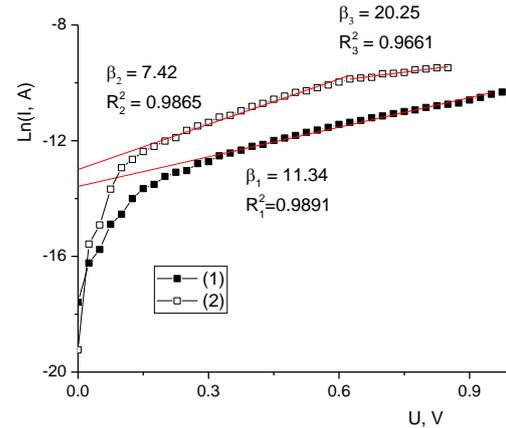
Fig. 3 – Forward-bias portions of the I-V characteristics of the Au/*n*-CdS (presented on the semilogarithmic scale): 1 – dark, 2 – lighting

Table 1 – Electrophysical parameters of dark Au/*n*-CdS SBS at room temperature

| Parameter	Value	Relative error
V_{bi}, eV	0.355	5.68%
R_s, kΩ	23.2	1.87%
I_0, µA	1.27	4.45%
β_1	11.34	2.36%
$q\Phi_{Bn}$, eV	0.436	1.32%

In the case of the SBS illumination by the solar radiation simulator, on the side of the barrier contact Au, (Fig. 3, curve 2), we observe two rectilinear portions of the *I-V* characteristic at a scale $lnI = f(U)$, indicating the exponential dependence and the presence of different dominant mechanisms of charge transport for different voltage ranges. In the region of low voltages

$\left(\dfrac{3kT}{q} < U < 0.6V \right)$ the ideality factor is $\beta = 7.42$ (see Table 2), which can be related to the tunneling-recombination nature of charge transport [4]. At higher voltages $U > 0.6$ V $U > 0.6\,V$ the ideality factor increases to $\beta = 20.25$, which indicates an increase in the contribution of the tunneling mechanism in the transport of charge [7].

Table 2 – Electrophysical parameters of the illuminated (1000 W/m²) Au/*n*-CdS SBS from the side of the barrier contact Au at room temperature

Parameter	Value	Relative error
V_{bi}, eV	0.250	5.34 %
R_s, kΩ	7.57	1.54 %
I_0, μA	2.27	5.79 %
β_2	7.42	3.02 %
β_3	20.25	6.57 %
$q\Phi_{Bn}$, eV	0.421	1.44 %

In the interval of the investigated reverse bias voltages ($U_{rev} < 1$V), there are two regions of power dependence between current and voltage $I \sim U^m$ (Fig. 4) for the dark and illuminated structure with close values of the slope of the corresponding linear sections of *I-V* characteristics. At the low voltages of reverse bias ($U_{rev} < 0.3$V), the exponent m is close to unity ($m_{2a} \approx 0.96$, Fig. 4), which is characteristic of tunneling of charge carriers or inherent to currents confined by the space charge in the saturation mode of the carrier rate [8].
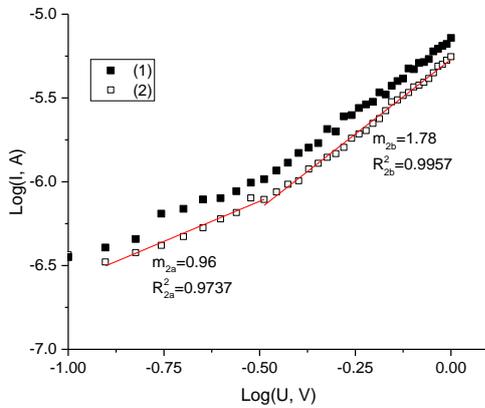
Fig. 4 – Reverse-bias portions of the *I-V* characteristics of the Au/*n*-CdS SBS on the logarithmic scale: 1 – dark, 2 – lighting

At higher voltages $U_{rev} < 0.3$ V, we observed an almost quadratic dependence $I \sim U^m$ ($m_{2b} = 1.78$) which is characteristic of currents confined by the space charge in the mobility mode [9].

The normal procedure for the test of materials for solar cell structure investigation is as follows:

1. Experimental measurements of the steady-state *I-V* characteristic of the test samples in the dark and under illumination, under forward and reverse bias.
2. Used differential technique for the *I-V* curve.
3. Analysis of the fine structure of the current in the *I-V* and α-V characteristics.

4. Recognition of the main injection and recombination regimes.

We have conducted experimental studies for materials to solar energy based on CdS thin films. For illustration, Fig. 5 presents the results of their differential treatment in the form of the α-V dependences.
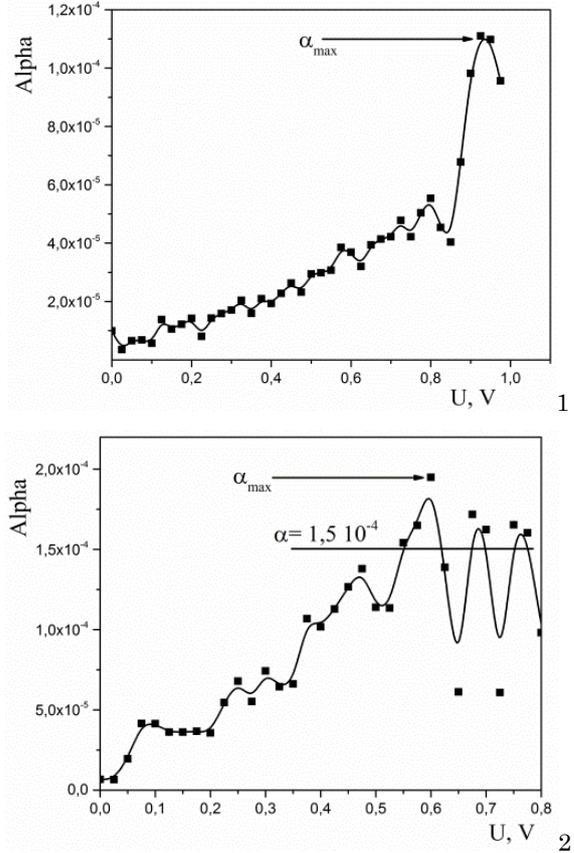
Fig. 5 – α-V dependencies obtained from I-V characteristics corresponding to curves CdS: 1 – for normal conditions; 2 – for illuminated by the simulator of sunlight

The behavior of the *I-V* characteristic can be approximated by different functional dependencies [10]. The results of differential treatment in the form of the α-V dependencies are presented in Fig. 5. Here we have a limit $\alpha_{max} < 1$ and, due to classification, it corresponds to mechanisms of injection and recombination [10] ($\alpha_{max} = 1.15 \cdot 10^{-4}$ for normal conditions and $\alpha_{max} = 1.9 \cdot 10^{-4}$ for illuminated by the simulator of sunlight). In the case of semiconductors, *I-V* characteristics are fitted most often by using the power (12), exponential (13) or logistic (14) functions. In the relations (12)-(14), x is voltage V and y is a corresponding electric current I. Other symbols in the relations (12)-(14) are the sample dependent parameters. An analysis of the mechanisms of injection and recombination of the charge carriers in a semiconductor is based on the diversity of behavior the injected charge carriers and their influence on *I-V* characteristic.

$$y = ax^n, \tag{12}$$

$$y = y_0 + A_1 e^{\frac{x}{t_1}}, \tag{13}$$

$$y = \frac{A1 - A2}{\left(1 + \dfrac{x}{x_0}\right)^p} + A_2 \qquad (14)$$

Approximation by the function (12) of the experimental I-V characteristic for CdS thin film for normal conditions at the room temperature is characterized by the coefficient of determination $R^2 = 0.889$. Here, the convergence of the calculated results to the experimental ones is not sufficient enough, therefore one can't assert about the possible mechanism of double injection [10] in the CdS thin film at normal conditions. However, with illumination by the simulator of sunlight, the convergence to the experimental dependence with the function (12) becomes better, $R^2 = 0.995$. This means that the double injection mechanism in CdS thin film for illuminated by the simulator of sunlight may appear [10].

Having analyzed the *I-V* characteristic by the functions (13) and (14), a much higher convergence has been obtained, $R^2 = 0.998$ (0.991) and $R^2 = 0.995$ (0.998) for normal conditions (for illuminated by the simulator of sunlight), respectively. It should be noted that for all samples, the convergence of the calculated results obtained using the functions (13) and (14) to the experimental data also increases. Therefore, one may adopt the weak injection and the constant field between contacts [10] as the prevailing modes in these cases.

Table 3 – Parameters of fitting calculated for the *I-V* characteristics of CdS thin film: R^2 is a coefficient of determination

| Function No	Parameters of function approximation	CdS at normal conditions	CdS for illuminated by the simulator of sunlight
1	a	$3.3 \cdot 10^{-5}$	$1.09 \cdot 10^{-4}$
	n	2.2	1.77
	R^2	0.889	0.995
2	y_0	$-3.02 \cdot 10^{-6}$	$-2.74 \cdot 10^{-5}$
	A_1	$2.88 \cdot 10^{-6}$	$2.44 \cdot 10^{-5}$
	t_1	0.39	0.56
	R^2	0.998	0.991
3	A_1	$8.11 \cdot 10^{-7}$	$1.47 \cdot 10^{-6}$
	A_2	0.07	$1.57 \cdot 10^{-4}$
	x_0	26.03	0.85
	p	2.35	2.59
	R^2	0.995	0.998

Our consideration of the charge carrier injection and recombination processes in test solar cell structures has shown that:

1. Thus, we have found that at room temperature the constant field between the contacts is the predominant modes in CdS thin film at normal conditions and for illuminated by the simulator of sunlight.
2. The weak injection is the predominant modes in CdS thin film at normal conditions, but the mechanism of double injection is the predominant modes in CdS thin film at illuminated by the simulator of sunlight.

Because CdS thin films are used as materials for the optical window of solar cells [1, 2], there is a need of identification of spectral region of transparency. For identification of spectral transparency of a sample we used photoconductivity spectra (PC). PC was measured using the monochromator MDR-23 with the spectral resolution of $\Delta\lambda \approx 1$ nm at room temperature. Measurements were carried out from the ITO surface direction. For excitation source, we used a halogen lamp.

The PC of CdS thin film at room temperature is presented in Fig. 6. The optical transparency of CdS thin film was observed at the wavelength region of 470-570 nm (at least in our experiment region). As can see, CdS thin films exhibit good optical quality. The absence of significant noise on the PC spectra confirms this.
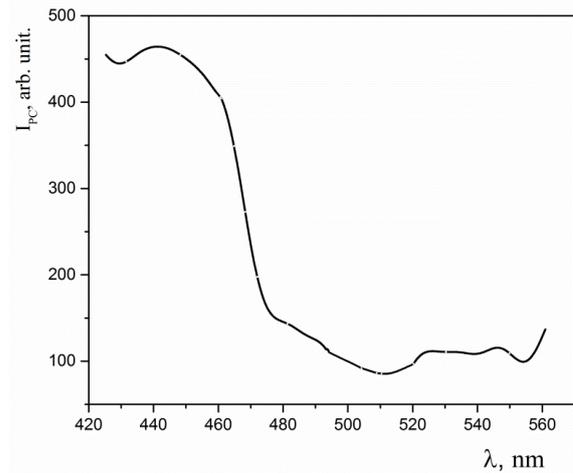
Fig. 6 – PC of CdS thin film at room temperature

To clarify the mechanism of PC for the CdS thin film near the absorption edge spectral region, we had recourse to the fact that the spectral dependence of photocurrent is generally consistent with the optical absorption spectrum for thin films. Taking into account that the peaks of spectral distribution of photoconductivity are responsible for the phototransitions in the thin film, one can evaluate the band gap energy E_g. It was found to be close to the value $E_g = 2.58$ eV estimated by the absorption band edge of the CdS thin film.

4. CONCLUSIONS

We studied the electrical properties of Au/n-CdS SBS produced by RF magnetron sputtering technique of CdS thin film and by application on a surface of CdS without its preliminary processing of a gold layer (Au) in thickness $h = 200$ nm.

The *I-V* characteristics of the dark and illuminated Au/*n*-CdS structure by the solar radiation simulator SF-150-C (1000 W/m²) from the side of the barrier contact Au were investigated. The basic parameters describing the stationary *I-V* characteristic of the Schottky contact are defined: the height of the barrier $e\Phi_{Bn}$ the ideality factor β, the series R_s resistance, the saturation current I_0, rectification factor k and built-in potential V_{bi}.

It is found from the analysis of the forward-bias portions of the I-V characteristics that the dominant mechanism of charge transport of the unlit (dark) SBS

is represented by multistage tunneling-recombination processes with the involvement of surface states at the metallurgical Au/n-CdS interface.

In the case of an illuminated structure, *I-V* characteristics in the coordinates $lnI = f(U)$ have two characteristic straight sections. In the range of low forward-bias voltages $\left(\dfrac{3kT}{q} < U < 0.6V\right)$ the dominant is tunneling-recombination mechanism of charge-carrier transport. At higher voltages $U > 0.6$ V, the contribution of the tunneling mechanism to the transport of charge carriers increases.

At reverse-bias voltages for the dark and illuminated structure, there are two regions of power dependence $I \sim U_m$ with close values of the parameters m. At low voltages of reverse bias ($U_{rev} < 0.3$ V), the dominant mechanism of charge transport is tunneling of charge carriers or inherent to currents confined by the space charge in the saturation mode of the carrier rate. At higher voltages $U_{rev} > 0.3$ V, we observe an almost quadratic dependence $I \sim U_m$ ($m_{2b} = 1.78$) which is characteristic of currents confined by the space charge in the mobility mode.

We have found that at room temperature the constant field between the contacts is presented in CdS thin film at normal conditions and for illuminated by the simulator of sunlight. The weak injection is the predominant modes in CdS thin film at normal conditions, but the mechanism of double injection is the predominant modes in CdS thin film at illuminated by the simulator of sunlight.

From the analysis of the photoconductivity spectrum, we found that the value of the absorption edge energy is approximately 2.58 eV for CdS thin film.

REFERENCES

1. R.Yu. Petrus, H.A. Ilchuk, A.I. Kashuba, I.V. Semkiv, E.O. Zmiiovska, *Opt. Spectrosc,* **126**, 220 (2019).
2. G.A. Il'chuk, V.O. Ukrainets, Yu.V. Rud', O.I. Kuntyi, N.A. Ukrainets, B.A. Lukiyanets, R.Yu. Petrus, *Tech. Phys. Lett.* **30**, 628 (2004).
3. Haynes W.M. (Ed.) *CRC Handbook of Chemistry and Physics 97th edition*. (CRC Press: Taylor & Francis Group: LLC: 2017).
4. S.M. Sze, K.N. Kwok, *Physics of Semiconductor Devices* (John Wiley: 2006).
5. Li S.S. *Metal-Semiconductor Contacts. In: Semiconductor Physical Electronics. Microdevices* (Springer: Boston: MA: 1993).
6. Li S.S. *Metal–Semiconductor Contacts. In: Semiconductor Physical Electronics* (Springer: New York: 2006).
7. M.N. Solovan, G.O. Andrushchak, A.I. Mostovyi, T.T. Kovaliuk, V.V. Brus, P.D. Maryanchuk, *Semiconductors* **52**, 236 (2018).
8. G.A. Il'chuk, V.V. Kusznezh, R.Yu. Petrus', V.Yu. Rud', Yu.V. Rud', E.I. Terukov, V.O. Ukrainets, *Semiconductors* **40**, 1321 (2006).
9. M. Lampert, P. Mark, *Current Injection in Solids* (New York: Academic Press: 1970).
10. R. Ciach, Y.P. Dotsenko, V.V. Naumov, A.N. Shmyryeva, P.S. Smertenko, *Sol. Energy Mater. Sol. Cells* **76**, 613 (2003).

Поверхнево-бар'єрні структури Au/*n*-CdS: створення та електрофізичні властивості

Р. Петрусь[1], Г. Ільчук[1], А. Кашуба[1,2], І. Семків[1], Е. Змійовська[1], Ф. Гончар[1], Р. Лис[2]

[1] *Національний університет "Львівська політехніка", кафедра загальної фізики, вул. Ст. Бандери, 12, 79013 Львів, Україна*
[2] *Львівський національний університет ім. І. Франка, факультет електроніки та комп'ютерних технологій, вул. Тарнавського, 107, 79005 Львів, Україна*

Представлено результати дослідження електрофізичних властивостей поверхнево-бар'єрних структур (ПБС) Au/*n*-CdS, одержаних ВЧ магнетронним розпиленням. Встановлено, що плівки кристалізуються в просторовій групі *P*63*mc*. Приводяться результати дослідження вольт-амперних характеристик (ВАХ) для неосвітлених та освітлених плівок. На основі поведінки ВАХ розраховано коефіцієнт ідеальності, висоту потенціального бар'єра зі сторони металу, струм насичення, послідовний опір структури, коефіцієнт випрямлення та висоту вбудованого потенціалу для темнової та освітленої структури. Встановлено, що коефіцієнт випрямлення в процесі освітлення ПБС Au/*n*-CdS імітатором сонячного випромінювання (1000 Вт/м²) зростає у порівнянні з темновою ВАХ від 3 до 22. Домінуючим механізмом переносу заряду, який встановлюється з темнових I-V характеристик напруг прямого зсуву, є багатоступеневі тунельні та рекомбінаційні процеси із залученням поверхневих станів на металургійний інтерфейс Au/*n*-CdS. Для освітленої прямої ВАХ за зміщень < 0,6 В переважає тунельно-рекомбінаційний механізм перенесення заряду, а за зміщень > 0.6 В – зростає внесок механізму тунелювання. При зворотному зміщені для темнової та освітленої ВАХ за зміщень < 0,3 В домінуючим механізмом струмопроходження є тунелювання носіїв заряду або ж струм, обмежений просторовим зарядом у режимі насичення швидкості, а за зміщень > 0,3 В – струм, обмежений просторовим зарядом в режимі рухливості. Результати дослідження фотопровідності (ФП) дозволили оцінити пропускну межу та ширину забороненої зони отриманої плівки.

Ключові слова: Метод магнетронного напилення, Тонкі плівки, CdS, Бар'єр Шотткі, Фотопровідність.